

CFD Study of Cooled Flow in Annular Combustor of Aircraft-Engine

Dhirgham Alkhafaji¹, Noor Al-Rubaye² and Mohammed Al-khafajiy³

¹ College of Engineering, Babylon University, Babylon/Iraq

² College of Engineering, Al Mustaqbal University Collage, Babylon/Iraq

³ Faculty of Engineering & Technology, Liverpool John Moores University, Liverpool/UK

Abstract: A three and two-dimensional numerical study is conducted to investigate the isothermal flow field in a model gas turbine combustor. CFD techniques of standard $k - \epsilon$ turbulence model used to analysis flow characteristic in annuals and dump cavity between pre-diffuser and liner dom. Flow feature investigated by 2D model, and creating 90° and 180° section on 3D model. Result shows the 2D and 3D models well agree with experimental result which investigated by J. F. carotte. The pressure loss coefficient; C_L recorded the average values 0.377, 0.431, and 0.397 in dump cavity, outer annuli, and inner annuli respectively. Cooling holes of the right and left side shows different rate of axial velocity rate. Turbulence intensity averaged 21.5%, 15% and 17% of IT in dump cavity, inner and outer annuli respectively. The above results productive by CFD code matching with media of flow and combustion in pre-diffuser-combustor system which mentioned in the combustor literature.

Keywords: - Annular combustor, CFD, Aircraft engine, Annulus flow, static pressure coefficient, Turbulence intensity.

1. Introduction

The development of the gas turbine engine as an aircraft power plant has been so rapid that it is difficult to appreciate that prior the 1950s very few people had heard of this method of aircraft propulsion. A combustion chamber is the most heavily thermal load part in an aero engine, in which both ignition and combustion keep going on, and normally whose service life is very short. Performance of the combustor flow and cooling air are parameters of combustor design. Since very limit data can be obtained from expensive engine tests due to its serious work environment, CFD is often employed to simulate the complex physical processes in a chamber. So far there are very plenty of available researches to validate the reliability of CFD analyses for investigating the flow, combustion and heat transfer in a combustor. As powerful computing technologies are continuously and rapidly improved, the feasibility of using CFD analyses is undoubted for combustor design. Many researchers [1-11] employed different model and CFD methods using commercial code to capture the axial, swirl flow and combustion flams. The research [18-24] using CFD analysis to study the reacting flow within the combustor tube, Crocker et al. [18] conducted a numerical analysis of an entire combustor domain, including the fuel nozzle, dome, inner and outer diffuser passages, and the dilution holes. Eccles and Priddin [19] also demonstrated the capability of full-combustor structured-mesh analysis, and highlighted the usefulness of a streamlined CAD-to-grid process utilizing parametric solid models. Birkby et al. [20] developed a description of an analysis of an entire industrial gas turbine combustor, in which the premixing fuel nozzle was coupled with the combustion chamber. Pratt and Whitney Corporation [21,22] developed a CFD analysis on an entire PW6000 combustor domain to predict temperature distribution at the combustor exit and compared the CFD results with

the full annular rig-test data. However, all above-mentioned studies on “full combustor” omitted cooling devices or simplify cooling holes to slots.

The demand for modern gas turbines with higher thermal efficiencies has greatly prompted designers to increase the turbine inlet gas temperatures steadily. One thousand and nine hundred Kelvin is a typical combustor inlet temperature for current aero-engine designs [23], which is well above the sustaining temperature of the tube material.

One method of protecting combustor tube in these harsh environments is discrete holes film cooling. The cooling air/fluid is injected through small discrete holes into the tube internal boundary layer, forming a protective film on the surface. Film cooling is widely used in the modern gas turbine combustors [19,22,23] to cool and protect tube walls and was extensively studied [14-18] in last 30 years. However, most of the researches in the open literature just concentrated on flat or curve plates with film injection through slots or rows of cylindrical holes, very few consider the integration of combustor and full film cooling. Here, authors tried to investigate the flow interaction between diffuser and an annular combustor and flow annulus which effected film cooling inside the liner. The entire calculation domain of the combustor contains 3D region from the pre-diffuser inlet to combustor exit, totally having 93 discrete film cooling holes. The simulated inlet and exit pre-diffuser velocities profile was compared with the results of J. F. Carrotte, *et al.* [29] to validate the reliability of commercial CFD cod analysis for predicting the feature of the flow in a gas turbine combustor. Flow characteristics inside combustor show that majority of loss between diffuser exit and entrance of annulus associated with high turbulence in this zone. Static pressure rises around the head of flame tube, which gives uniform flow through cooling holes and cooling film, can be formed along the walls of the flame tubes, however, on the rear edge of the dilution holes the film would be destroyed by the strong injected airflow, which makes very high temperature areas appear near the dilution holes. The complex geometry of annular combustor of aircraft engine which tested by Carrotte used to analysis by using commercial code FLUENT6.1.

2. Model Description

2.1. Geometry and Grid

The combustor model was created by Gambit drawing software and exported to CFD solver Fluent6.1. Fig.1 show the combustor assembly consists various parts and small design details, such as pre-diffuser, flame tube(liner), and buckets of cooling holes. The inlet of combustor diffuser system passage height ($h_1= 36.6$ mm). The geometry configuration details on the following ratios; Pre-diffuser exit height($h_2/h_1=1.35$), Inner annulus height ($h_i/h_1=1.41$), outer annulus height ($h_o/h_1= 0.67$), flame tube radial depth ($D/h_1= 5.5$), dump gap distance ($L/h_2=1.0$).The geometrical clean up from some attached parts and small details which do not significantly affecting the fluid flow and necessary for simplifying the processes of 3-D model creation and mesh generation Fig.2. The simulative domain adopted here is 93 discrete tiny film cooling holes distributed on the inner and out flame tubes are maintained for fully exploring the performance of the film cooling. There are three rings of film cooling holes in 31 rows on the inner/outer tubes, along the fluid flow direction. The tiny film cooling holes are nearly equal-spaced along the span wise direction and cover the whole tubes with an average diameter of about 3.826 and 10.627 mm, there are also one row of the dilution holes on the outer and inner, respectively. The diameter of the dilution holes is 3.826 mm. Unstructured Tet-hybrid meshes were used for this simulation computation. These meshes contained 247,303 nodes and 1,239,071elements. Grid densities for different components of the geometry were specified to obtain maximum resolution of the corresponding components.

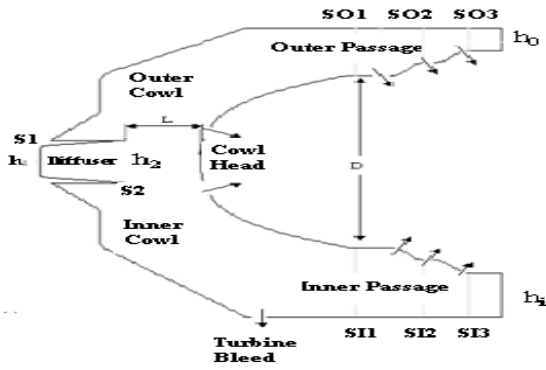


Fig 1: Combustor model details

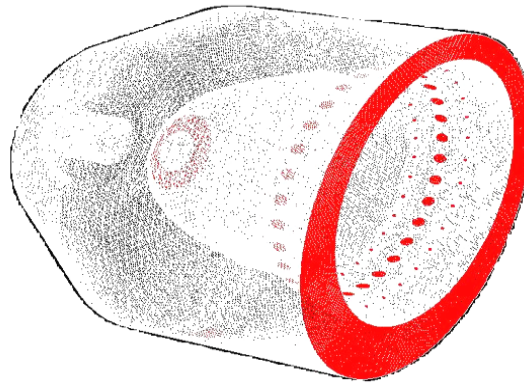


Fig 2: Grid mesh generation on the model

2.2. Boundary Conditions and Flux Distribution

The boundary conditions of the flow and their direction are summarized in Fig.1. Mass flow split to outer feed annulus 24.3%, inner feed annulus 20.6%, turbine bleeds passage 6.4%, flame tube head 48.7%. The flow, having passed through the combustor was expelled to atmosphere.

3. Modeling and Mathematical Formals

Initially the flow is assumed to be steady, isothermal, and turbulent. The fluid flow through the combustor is the air. The following governing equations were solved for fluid dynamic model:

$$\text{Continuity Equation: } \frac{\partial \rho}{\partial t} + \nabla \cdot (\rho \mathbf{U}) = 0 \quad (1)$$

$$\text{Momentum Equation: } \frac{\partial (\rho \mathbf{U})}{\partial t} + \nabla \cdot (\rho \mathbf{U} \otimes \mathbf{U}) = \nabla \cdot (-p \delta + \mu (\nabla \mathbf{U} + (\nabla \mathbf{U})^T)) + S_M \quad (2)$$

Where ρ , p represent density and static pressure, respectively, \mathbf{U} velocity vector of $U_{x,y,z}$, μ turbulent viscosity, and S_M momentum source. For this application, the review infers that standard ($k-\varepsilon$) model is more suitable for this turbulence characteristics and fluid flow physics [12].

3.1. Standard $k-\varepsilon$ Model

The turbulence kinetic energy, k and its rate of dissipation, ε , are obtained from the following transport equations:

$$\frac{\partial}{\partial t} (\rho k) + \frac{\partial}{\partial x_i} (\rho k v_i) = \frac{\partial}{\partial x_j} \left[\left(\mu + \frac{\mu_t}{\sigma_k} \right) \frac{\partial k}{\partial x_j} \right] + G_k + G_b - \rho \varepsilon - Y_M + S_k \quad (3)$$

$$\begin{aligned} \frac{\partial}{\partial t} (\rho \varepsilon) + \frac{\partial}{\partial x_i} (\rho \varepsilon v_i) &= \frac{\partial}{\partial x_j} \left[\left(\mu + \frac{\mu_t}{\sigma_\varepsilon} \right) \frac{\partial \varepsilon}{\partial x_j} \right] \\ &+ C_{1\varepsilon} \frac{\varepsilon}{k} (G_k + C_{3\varepsilon} G_b) - C_{2\varepsilon} \rho \frac{\varepsilon^2}{k} + S_\varepsilon \end{aligned} \quad (4)$$

In these equations, G_k represents the generation of turbulence kinetic energy due to the mean velocity gradients, Y_M represents the contribution of the fluctuating dilatation in compressible turbulence to the overall dissipation rate, $C_{1\varepsilon}$, $C_{2\varepsilon}$, and $C_{3\varepsilon}$ are constants. σ_k and σ_ε are the turbulent Prandtl numbers for k and ε , respectively. S_k and S_ε are source terms.

3.2. Turbulence Viscosity:

The turbulent viscosity, μ_t , is computed by combining k and ε as follows: Where C_μ is constant.

$$\mu_t = \rho C_\mu \frac{k^2}{\varepsilon} \quad (5)$$

The model constants $C_{1\varepsilon}, C_{2\varepsilon}, C_\mu, \sigma_k$ and σ_ε have the following values:

$C_{1\varepsilon} = 1.44, C_{2\varepsilon} = 1.92, C_\mu = 0.09, \sigma_k = 1.0$ and $\sigma_\varepsilon = 1.3$, these values have been determined from experiments with air for fundamental turbulent shear flows.

3.3. Performance Flow Parameters

The parameters investigated in this paper are the most frequently used factors of the combustor flow performance are static pressure recovery coefficient C_p , total pressure loss coefficient C_L and turbulence intensity IT. The static pressure recovery is defined as the ratio of static pressure rise through diffuser to the inlet dynamic pressure:

$$C_P = \frac{P_{s2} - P_{s1}}{P_{t1} - P_{s1}} \quad (6)$$

The stagnation pressure loss coefficient is defined as the ratio of loss in total pressure to the inlet dynamic pressure:

$$C_L = \frac{P_{t1} - P_{t2}}{P_{t1} - P_{s1}} \quad (7)$$

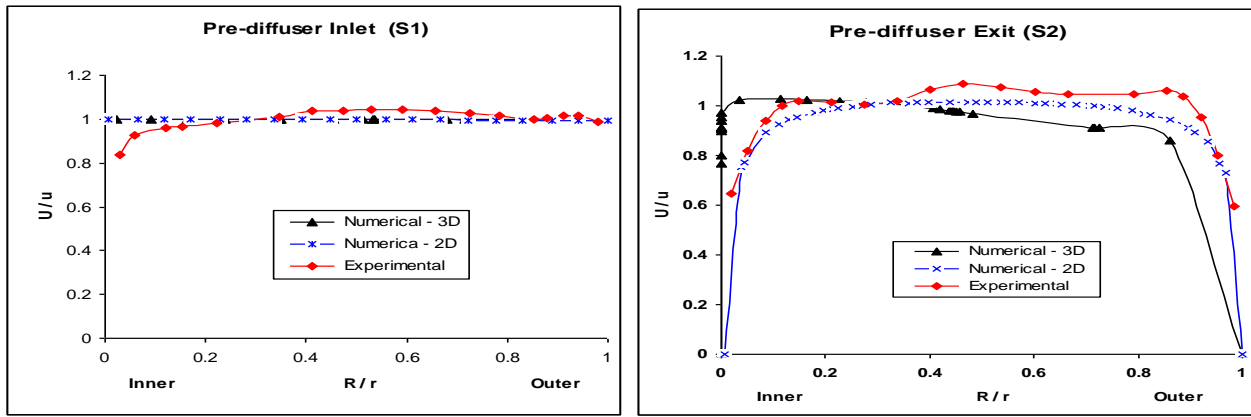
where “1” and “2” denote upstream and down stream planes respectively. The turbulence intensity is one of the key factors for combustor performance. The turbulence intensity is most frequently defined as in RMS value:

$$TI = \frac{\left[\frac{1}{3} (u'^2 + v'^2 + w'^2) \right]^{1/2}}{U} \quad (8)$$

Where $u' = (u^2)^{1/2}$ is the RMS of the velocity fluctuation in the U-direction, etc. U is assumed to be mean flow velocity in the direction of the diffuser. Equation (8) defines the parameter most frequently used to specify the overall level of turbulence intensity.

4. Validation of CFD Code

Preliminary investigations carried out for validation of CFD code with experimental results of J.F. Carrotte, *etc.* [29] shown in Fig.3. For local investigation of a various stages, namely S1 and S2 are located in between the pre-diffuser inlet and exit. Axial velocity normalized to the mean inlet velocity (u/U) and radial distance normalized to the combustor radius (r/R). The non-dimensional axial velocity plotted against non-dimensional distance along pre-diffuser inlet and exit. The radial distribution of the flow at inlet (S1) and exit (S2) from the pre-diffuser are clearly indicate by the circumferentially average axial velocity profiles for experimental, computational 2D, and 3D models. The variation of axial velocity profile in the flow direction at pre-diffuser inlet and exit are shown in Fig.3 (a), (b). Predictions using CFD cod Fluen6.3 shows better agreement with experiments for both 2-D and 3-D models. The profiles of axial velocity at pre-diffuser exit of the 3-D remark more matching with the experimental velocity profile.



(a)

(b)

Fig 3: Axial velocity profile. (a) Inlet of pre-diffuser. (b) Exit of pre-diffuser.

5. Results and Discussion

For optimum flow characteristics, many flow performance parameters are investigated at CFD model. The results followed by the 3-D and 2-D simulations and the post process calculations are lay on converging of mass flow rate 4.6 kg/s through diffuser combustor system models. The converges of 10^{-6} residual accuracy for continuity equation, x-velocity, y-velocity, z- velocity, k, and ϵ war done. The CFD analysis of 3-D combustor model predicted the air flow characteristics; axial velocity vector and contours plot Fig.4 shows the prediction flow field along the horizontal plane (180° section), and vertical plane (90° section) of 3-D combustor model. Air discharged from the pre-diffuser; split into three branches: two streams that feed the inner and outer combustor annuli and a third that supplies air to the combustor dome. Because of the flow expansion, two recirculation zones form at the corners in the dump region. The lower recirculation zone is stronger than the upper one. Further, there is substantial nonuniformity in the velocity distributions in the annuli. A small amount of the flow split to the bleeding hole from the inner passage. The cross flow accelerated fast through the outer passage cooling holes than inner passage holes, this will help to achieve a good mixing of cool flow with hot flow jet in side the liner. The velocities at pre-diffuser exit, dump zone, annuls entrance, and at first row of cooling holes are ranged about 66%, 54%, 5%, and 10% of the inlet velocity respectively. Several authors have noted how the performance of a diffuser-combustor system varies with inlet conditions [15].

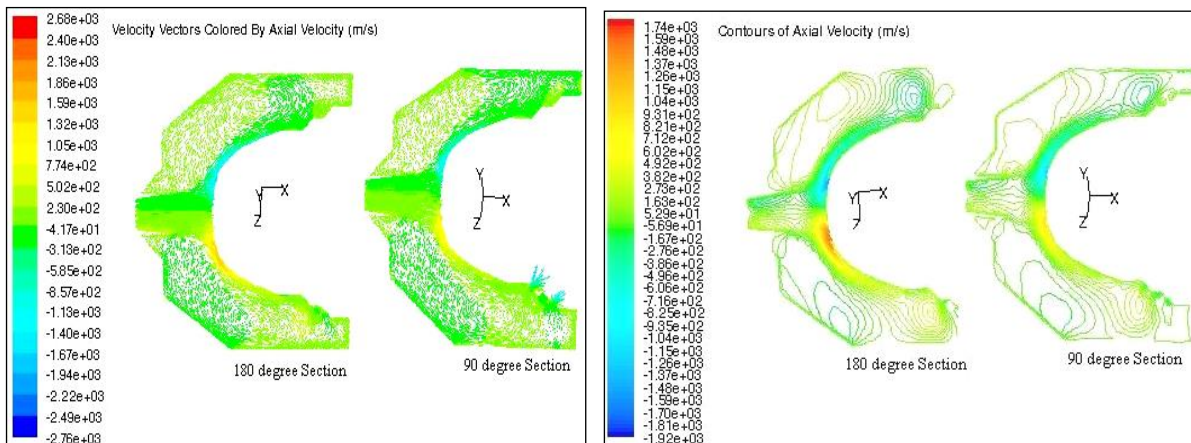


Fig 4: Axial velocity vectors and contours plot on horizontal and vertical plan of 3-D Model.

5.1. Annulus Flow Feature

For investigate the annuli flow characteristics and across flow of the cooling holes, three stations on the upper side SO1, SO2, SO3 and for lower side SI1, SI2, SI3 are marked as in investigated stages Fig.1. A computational study indicates decrease of velocity is about (5-10%) between pre-diffuser exit and annulus entrance. It is the high-velocity gradients in this region where a significant amount of turbulence and hence stagnation pressure loss, is generated [8]. At entry to each feed annulus the flow distribution is still biased toward the flame tube, to the outer and inner feed annuli by the circumferentially average axial velocity profile station SO1, SO2, SO3 and SI1, SI2, SI3 on the outer and inner annuli respectively shown on fig.5. The axial velocity profiles computed for the flow passing downstream stations on the outer and inner annulus show similar profile on all station; only for station SI1 show increasing with the velocity compering with SO1 as shown in Fig.5. The velocity increasing of SI1 due to the air gravity and the bleeding hole which located on inner side.

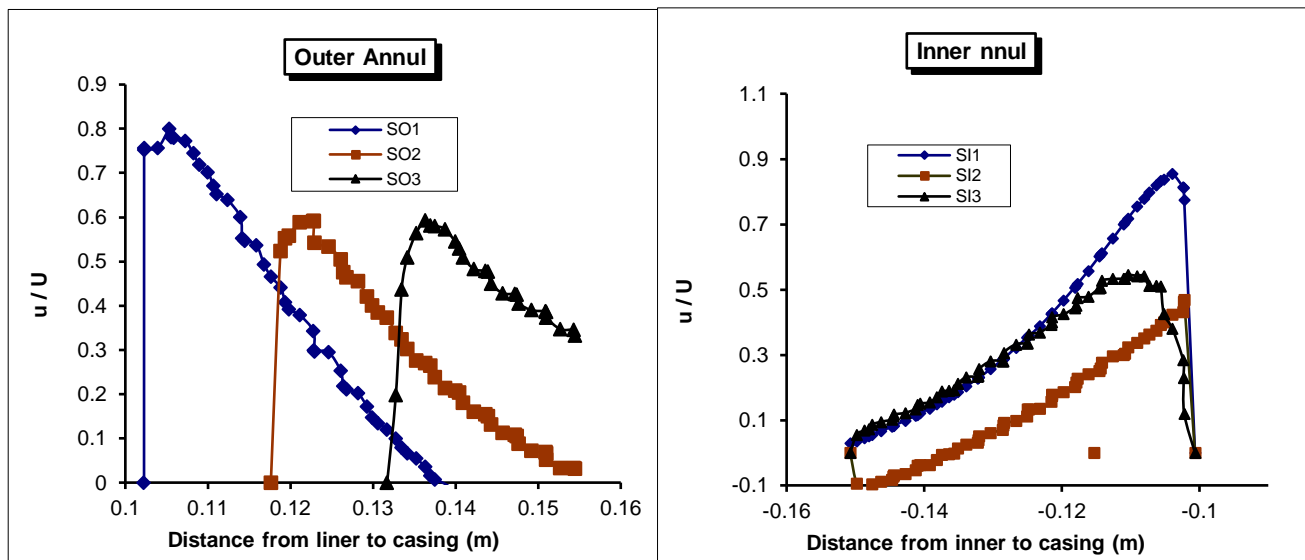


Fig 5: Outer annulus and Inner annulus velocity profiles

5.2. Air Film Cooling on Annular Tubes

Thermal protection of flame tube walls is very important to prolong engine life. The combustor is cooled and/or thermally protected by full discrete tiny holes film cooling. When chilly air is injected into the flame tube the tiny holes on its outer and inner walls, a film layer formed adjacent to the inner side of the tube wall Fig.6. The film separates the flame and/or hot gas from the tube wall and greatly attenuates the convection and radiation heating of the tube wall from the hot gas. These effects can efficiently protect the high thermo-load tube wall from overheating. In addition to these, the discrete tiny cooling holes can also abate thermal stress and deformation.

5.2.1. Cold Flow Performance along Pre-Diffuser Combustor Interaction

Fig.6 display the velocity contours on axial section strip form the headliner (cowl head) and the three ring of cooling holes on several typical outer and inner passage strips in axial cross-section. The flow behavior at each bend of the film cooling holes varies as shown in Fig.6, elevated level of velocity for flow attached to the right-side liner surfaces on the liner head, first and third bend of cooling holes compering with left side on both the outer and inner tube, because the complex annulus geometry, circumferential flow and jet angle of through the cooling holes, which located in different angle bend around liner surface. The CFD study predication for cross-flow injection inside the liner with different magnitudes and directions of axial flow from cooling hole Fig.7. The predication flow shown inFig.7 supported the literature mentioned by Lefevre, A.H [30]. That cross-flow

support swirl flow in side liner to achieve a good fuel air mixing, and in addition to protected the liner wall by chilly air flam.

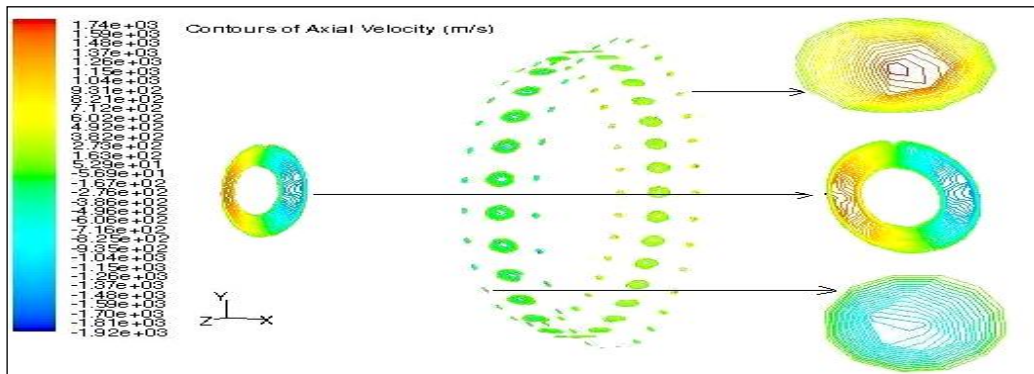


Fig 6: Axial velocity contours of chilly air through holes.

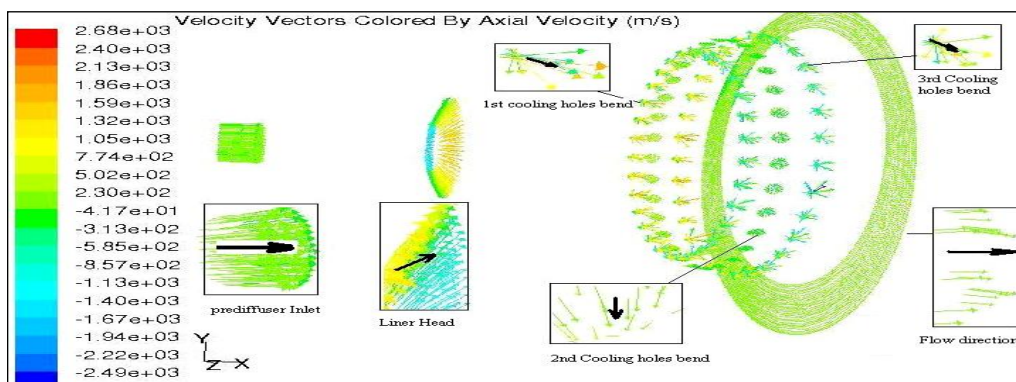


Fig 7: Flow direction of velocity of different strips

5.3. Static Pressure Contours Distribution

The flow accelerates around the head, away from the stagnation point, giving rise to high velocities adjacent to the cowl surface. This is reflected by the static pressure, which remarkable rises in the dump gap at the exit of pre-diffuser and concerted on the flam tube head. The flow taken place around curvature of the liner head to the annulus the boundary layer growth on the combustor wall to indicate the static pressure rises on the combustor wall shown in vertical and horizontal section of combustor model Fig.8.

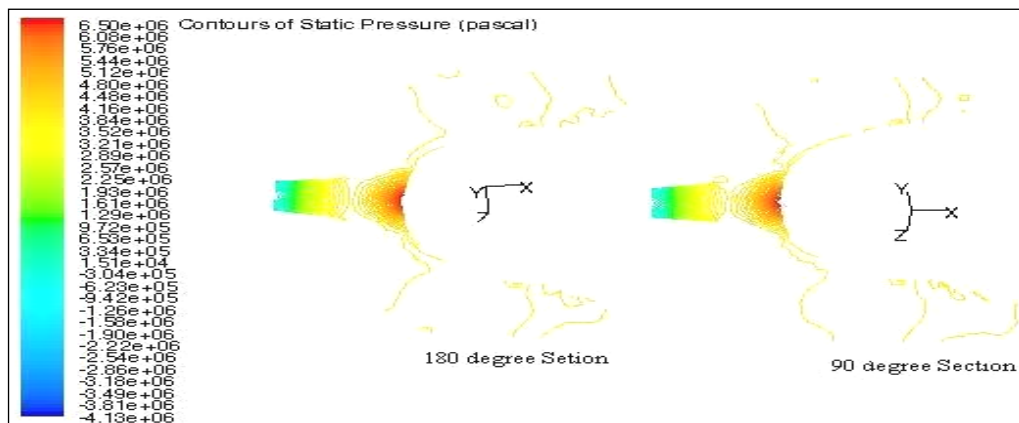


Fig 8: Static pressure contours distribution on combustor model

5.4. Performance Parameters of the Flow

Pressure Recovery (C_p), pressure Loss (C_L) Coefficients, and Turbulence intensity (IT) are remarked as aerodynamic performance parameters of combustor flow. Generally, pressure decreases rapidly to a minimum before undergoing a rise in pressure prior to entering each feed annulus. Based on the definition of (C_p), (C_L), and (IT) are computed for all stations along diffuser combustor system and listed in table .1. The pre-diffuser static pressure recovery coefficient 0.354 is sizable proportion of the total static values of 0.505 and 0.499 recorded between pre-diffuser inlet and outer (SO3) and inner (SI3) feed annuli. Although there is a relatively large velocity reduction between pre-diffuser exit about 28% and feed annuli about 77%, the static pressure rise is significantly reduced by the relatively high stagnation pressure loss around the flame tube head. It can therefore be seen that in terms of overall diffuser performance, most of the static pressure rise occurs within the diffuser

The stagnation pressure losses between pre-diffuser inlet (S1) and outer (SO3) and inner (SI3) feed annuli are 0.495 and 0.403, respectively. Since the loss within pre-diffuser is 0.368, this implies that a substantial proportion of loss occurs downstream of pre-diffuser as the flow passes around the flame tube head and enters feed annuli. It is also interesting to note the relatively high stagnation loss of 0.335 that is associated with the flow passes entering the turbine bleed passage. This represents low-energy high-loss flow that is drawn through the bleed ports from the inner dump cavity. The remaining flow passes to the inner annulus and so, by removing low-energy air, this may account for the relatively low loss within this annulus relative to the outer feed annulus. In general, the pressure loss coefficient recorded the average values 0.377, 0.431, and 0.397 in dump cavity, outer annuli, and inner annuli respectively.

In combustion media always required some amount of turbulence level for improved mixing and distribution of mass in the combustion region. Based on deficient of turbulence intensity, and inlet condition of $TI=3\%$. The following features in table.1 are highlighted two zones:

(i) Low turbulence zone: it is concentrated on the pre-diffuser exit and cowls of 6% TI, and averaged about 12.5% in the dump cavity.

(ii) High turbulence zone: highly of turbulence intensity is concentrated in the dump cavity around dome surface and the entrance of feed annulus is about 21.5% of turbulence intensity. The turbulence decreases in direction of flow to feed annulus. It is averaged 17% in outer annuli and 15% in inner annuli. The outer annuli show slightly increase of the turbulence comparing with inner annuli because the relaxations of fluid diffusion in inner annuli.

TABLE I: The Coefficients of Pressure Recovery (C_p), Pressure Loss (C_L), and The Turbulence Intensity Along Pre-Diffuser-Combustor System.

| Station | Performance Parameter | | |
|----------------------|-----------------------|-----------|--------|
| | C_p (%) | C_L (%) | IT (%) |
| Pre-diffuser exit | 35.4 | 38.6 | 06 |
| Dump gape | 51.4 | 41.2 | 15.6 |
| Turbine bleed | 39.6 | 33.5 | 15.8 |
| Outer annulus, (SO1) | 48.5 | 39.4 | 23.0 |
| (SO2) | 50.3 | 40.5 | 18.0 |
| (SO3) | 50.5 | 49.5 | 05.0 |

| | | | |
|----------------------|------|------|------|
| Inner annulus, (SI1) | 47.3 | 38.6 | 20.0 |
| (SI2) | 49.8 | 40.2 | 16.0 |
| (SI3) | 49.9 | 40.3 | 06.0 |

6. Conclusions

A computational investigation has been undertaken on modern dump diffuser system with inlet conditions being generated by an axial flow. Computational determine using $k - \varepsilon$ turbulence model obtained at a dump gap of 0.1. The following conclusions have been drawn:

- The CFD technique using $k - \varepsilon$ turbulence model useful tool for analysis flow in such complex geometry like combustor. Results of two and three-dimensional models give reasonable agree with experimental data.

- The stagnation pressure loss coefficient C_L between pre-diffuser inlet and the outer and inner feed annuli were 0.495 and 0.403 respectively. The majority of loss was generated around of the flame tube head while most of the static pressure rise occurred within the pre-diffuser.

- Cooling holes of the left side show more of axial velocity rate comparing with corresponding holes within right side. Mass flow rate from inner holes more than outer holes with similar constant contours distribution of the axial velocity.

- Turbulence increasing from pre-diffuser to the dump cavity and entrance of feed annulus averaged 20.5% of IT. Turbulence decrease within annulus, it is averaged 14% and 15.3% in the inner and outer annuli respectively.

7. References

- [1] H. Naitik, Gor, J. and Milan Pandey. "CFD analysis of swirl can combustor chamber-A review," *IJIRST*, vol.1, Iss 6, November. 2014.
- [2] F. Luis, M. Antonio, ...etc. "Reference area Investigation in a gas turbine combustion chamber using CFD, " *J. of Mechanical Engineering and Automation*, vol. 4, iss 2, pp.73-82, 2014.
<https://doi.org/10.5923/j.jmea.20140402.04>
- [3] D. Alkhafaji, W. Alqaraghuli, and A. Shires. "Simulation of the flow inside an annular can combustor". *International Journal of Engineering & Technology*, vol. 3, iss 3, pp. 357-36, 2014.
- [4] I. Yang, Y. Ji Lee, and K. Jae Lee "Effect of Combustor Configuration on Flow and Combustion in a Scramjet Engine" *Journal of propulsion and power*, vol. 29, No. 3, May-June. 2013.
<https://doi.org/10.2514/1.B34737>
- [5] P. Gobbal, Massimo Mas,.... atc. "Calculation of the flow field and NO_x emissions of a gas turbine combustor by a coarse computational fluid dynamics model" *.Elsevier; J. of Energy*, vol. 45, Iss. 1, pp. 445-455, September 2012.
- [6] R. A., D. Alkhafaji, P. Talukder "Effect of Casing geometry on the Flow characteristics in a model Can-Combustor". ASME Conference "Gtindia2012" in *Mumbai, Maharashtra, India, Dec. 1, 2012*.
- [7] B. S. Mohammad and S. M. Jeng "Gas Turbine Combustor Sector Flow Structure" *Journal of propulsion and power*, vol. 27, No. 3, pp. 710-717, May-June 2011.
<https://doi.org/10.2514/1.B34114>
- [8] M. Masi, P. Gobato, A. Toffolo, A. Lazzaretto, and S. Cocchi "Numerical and experimental analysis of the temperature distribution in a hydrogen fueled combustor for a 10 MW gas turbine". *J Eng Gas Turb Power*, vol 2, pp. 133, 2011
- [9] A. Rahim, S. N. Singh, , and S. V. Veeravalli, "Liner dome shape effect on the annulus flow characteristics with and without swirl for a can-combustor ", *J. Power and Energy, IMech*, vol.221, Part A, 2007.

- [10] P. Moin and S. V. Apte. "Large-Eddy Simulation of Realistic Gas Turbine Combustors", *AIAA Journal*, vol. 44, pp. 698-708, 2006.
<https://doi.org/10.2514/1.14606>
- [11] A. Rahim., S.V. Veeravalli, and S. N. Singh, "Effect of inlet swirl and dump-gap on the wall pressure distribution of a model can-combustor". *Indian J. Eng. Mater. Sci.*, vol. 9, pp. 472–479, 2002,.
- [12] G.J. Sturgess, R. McKinney, and S. Morford, "Modification of combustion stoichiometry distribution for reduced NOx emission from aircraft engines", *ASME paper 92-GT-0108*, 1992.
- [13] T.C.J. Hu, and L.A. Prociw, "Recent CFD applications in small gas turbine combustion systems development, in: Proc. 81st Symp. Propulsion and Energetic Panel on Fuels and Combustion Technology for Advanced Aircraft Engines", in Rome, Italy, *AGARD Conference*, 1993.
- [14] M.S. Anand, J. Zhu, C. Connor, and M.K. Razdan, "Combustor flow analysis using an advanced finite volume design system", *ASME Paper 99-GT-0273*, 1999.
- [15] T. Behrendt, C. Martin, and C. Fleing, "Experimental and numerical investigation of a planar combustor sector at realistic operating conditions", *ASME Paper 2000-GT-0123*, 2000.
- [16] S.M. Cannon, V. Adumitroaie, and C.E. Smith, "3D LES modeling of combustion dynamics in lean premixed combustors", *ASME Paper 01-GT-0375*, 2001.
- [17] V. Smililjanovski, and N. Brehm, "CFD liquid spray combustion analysis of a single annular gas turbine combustor", *ASME Paper 99-GT-0300*, 1999.
- [18] D.S. Crocker, D. Nickolaus, and C. Smith, "CFD Modeling of a gas turbine combustor from compressor exit to turbine inlet", *ASME Paper 98-GT-0184*, 1998.
- [19] N.C. Eccles, and C.H. Priddin, "accelerated combustion design using CFD", *XIV ISABE*, pp. 99-7094, 1999.
- [20] P. Birkby, R.S. Cant, Dawes, and W.N., "CFD analysis of a complete industrial lean premixed gas turbine combustor", *ASME paper 2000-GT-0131*, 2000.
- [21] R.E. Malecki, C.M. Rhie, and R.G. McKinney, "Application of an advanced CFD-based analysis system to the pw6000 combustor to optimize exit temperature distribution—Part I: description and validation of the analysis tool", *ASME paper 2001-GT-0062*, 2001.
- [22] T.S. Snyder, and J.F. Stewart, "Application of an advanced CFD-based analysis system to the pw6000 combustor to optimize exit temperature distribution—Part II: predications of full annular rig test data", *ASME paper 2001-GT-0064*, 2001.
- [23] S.Y. Ge, "Film Cooling, Science Publishing Company", pp. 16–17, 1985.
- [24] A. Brankovic, A. Mckinney, and M. Colket, "Comparison of measurements and predictions of flow in a gas turbine engine fuel nozzle", *AIAA paper 2000-0331*, 2000.
<https://doi.org/10.2514/6.2000-331>
- [25] M.A. Paradis, "Film cooling of gas turbo turbine blades, a study of the effect of large temperature difference on film cooling effectiveness", *J. Eng. Power Trans. ASME 99*, sec. A, No. 1, pp. 11–20, 1970.
- [26] E. Lutum et al., "An experimental investigation of film cooling on a convex surface subjected to favorable pressure gradient flow", *Int. J. Heat Mass Transfer 44*, pp. 939–951, 2001.
[https://doi.org/10.1016/S0017-9310\(00\)00158-7](https://doi.org/10.1016/S0017-9310(00)00158-7)
- [27] Y. Yu, and C.H. Yen, "Film cooling effectiveness and heat transfer coefficient distributions around diffusion shaped holes", *ASME J. Heat Transfer 124*, pp. 820–827, 2002.
<https://doi.org/10.1115/1.1418367>
- [28] Y.Z. Lin, and B. Song, "G.E Liu, Investigation of film cooling effectiveness of full-coverage inclined multi hole walls with different hole arrangements", *ASME paper 2003-GT-38881*, 2003.
- [29] L. Li, X.F. Peng, and T. Liu, "Combustion and cooling performance in an aero-engine annular combustor", *ELSEVIER, Applied Thermal Engineerin*, 2006.
- [30] J. F. Carrotte, , Bailey, D. W., Frodsham, and C. W. "Detailed Measurements a modern combustor dump diffuser system". *ASME, J. of Engineering for Gas Turbine and Power*, vol. 117, pp 678-685, October 1995.
<https://doi.org/10.1115/1.2815453>

[31] Lefevre, and A.H., "Gas turbine combustion", *Hemisphere Publishing Corporation*, in Washington, 1983.

[32] Finshenden, C. R., and Stevens, and S. J. "Performance of annular combustor dump diffuser". *J. Of Aircraft*, vol. 14, no.1, 1977.